Journal of Applied Polymer Science

Tracking the chemical surface properties of racemic thalidomide and its enantiomers using a biomimetic functional surface on a quartz crystal microbalance

Acharee Suksuwan,[1] Luelak Lomlim,[1] Franz L. Dickert,[2] Roongnapa Suedee[1]

[1]Department of Pharmaceutical Chemistry, Faculty of Pharmaceutical Sciences, Molecular Recognition Materials Research Unit, NANOTEC Center of Excellence at PSU/Drug Delivery System Research Center, Prince of Songkla University, Hat Yai, Songkhla 90112, Thailand

[2]Department of Analytical Chemistry, University of Vienna, Währingerstrasse 38, A-1090 Vienna, Austria

Correspondence to: R. Suedee (E-mail: roongnapa.s@psu.ac.th)

ABSTRACT: We present details of the chemical surface properties of the molecularly imprinted polymer (MIP) on quartz crystal microbalance (QCM) for the tracking of the chiral recognition of racemic thalidomide and its (*R*)-enantiomer. We investigate the assembly and specific patterns of enantiomer and racemate of thalidomide on the poly(urethane) coating consisted of the synthetic-estrogen bisphenol A (BPA) on a QCM electrode by infrared spectroscopy and atomic force microscopy (AFM), which confirmed the surface properties of these materials. The BPA present on the surface of the coating layer revealed a positive frequency response for the racemic thalidomide that eventually appeared. This involved a negative shift of 80 Hz for a 200 μg mL^{-1} racemic thalidomide, and in all cases, a negative shift of 200 Hz for a 100 μg mL^{-1} (*R*)-thalidomide. The affinity constants (K_a) for the racemate adsorbed onto the polymer layer imprinted with (*R*)-thalidomide were lower than those for the (*R*)-thalidomide. Also, the binding energy involved a different binding process of the chiral forms and indicated that the two enantiomers had a twofold difference in their binding energies. Thus, the advantage of the use of BPA is proven that will function as hydrogen-bond donors in the enantioselective recognition site of the MIP. The data of functional analysis demonstrated that the biomimetic detection using molecular imprinting turn out to a study of the pharmaceutical effects of a pharmaceutically chiral compound on natural receptor functions. This approach is highly useful that highlight an enhanced understanding of the mechanism of stereochemistry required for biological controls.
 J. Appl. Polym. Sci. **2015**, *132*, 42309.

KEYWORDS: biomedical applications; biomimetic; molecular recognition; stereochemistry; tacticity

Received 7 May 2014; accepted 5 April 2015

DOI: 10.1002/app.42309

INTRODUCTION

One key advantage of molecular imprinting techniques is their ability to create recognition materials that can have antibody analogous interactions toward the target analytes.[1] These antibody-like bioselective reagents are also useful in biomedical applications, for example to detect therapeutics, or to evaluate the surface energetics of small organic molecules such as an active pharmaceutical ingredient (API). This organization of an artificial surface is a suitable and efficient method for creating bioselective reagents through incorporating small, pharmaceutically active compounds via noncovalent interactions. This methodology allows for an efficient recognition by molecular imprinting on a polymer and the binding of the original template to the cavities.[2]

There has been a growing interest, with an emphasis on the recognition process, by which the stereochemistry of an imprinted molecule is recognized by chirally specific molecular imprinted cavities within a layered material of a metal.[3] Molecularly imprinted polymerized polymers (MIPs) can be formed in the presence of a reversible sensitive template molecule that can subsequently be removed and leave a selective cavity within the polymeric matrix.[4] Over the years, bioassays using biopolymers, such as proteins, have offered opportunities within many scientific fields such as drug discovery/design[5] and the development of MIPs for the separation and/or analytical applications.[6] In addition, the chemical functionalization of the polymer and the chiral templating compounds allows for the determination of some of the physicochemical and stereochemical properties that are involved in drug delivery.[7] These selective imprinted materials, after adsorbing the specific target molecules, can enable the determination of the structural and dynamic interactions of the spatially defined sites.[8] The energetic advantage of this approach

is that it is possible to use some of these natural analogs to reconstruct the recognition of the biologically relevant substances, that have surface properties of the APIs and reflect the chemical environment of the surface. Therefore, the information of the chemical surface and energetic surface properties for APIs provides usefulness of their sorption process and interfacial phenomena in the development of formulation needed in the pharmaceutical process of manufacturing and industry.

One major important consequence of this technique is that it provides for the tracking of the chiral recognition through the assembly of the chiral template molecules on a polymerized network. This has also allowed for the fabrication of the polymer that surrounds the cavities that were complementary to the template structure that occur in a very straightforward way, so that the binding site of the imprinting polymer is employed efficiently for predicting the performance of the templating molecules or proteins.[9] The chiral entities can be precisely tailored in the sensor coatings onto the transducer system. The highly selective chemical sensors have utilized MIPs with specifically attracting motifs to rebind the desired isomer for the fabrication of a chiral imprint at the functional surface domains.[10] In combination with a mass-sensitive transducer, this would provide a model for the interactions between the probing molecules and the sensitive surface layer as a result of the sensor measurements.[11] The use of a quartz crystal microbalance (QCM) can be a powerful acoustic-based method for a precise chemical and surface characterization.[12] The target adsorption, measured by mass transfer diffusion, has been previously reported.[13] In addition, the surface-adsorbed molecule was induced with an adjustable chemical functional group that matched the biologically relevant entities on a defined recognition site in the polymeric macromolecular network.[14] The parameters that affected the template binding to the surface chemical functionalization turned out to provide for a study of the nature of the interactions at equilibrium.

The use of the quantum/statistical mechanical properties of the surface active material to devise methods for the characterization of the specific chemical properties of APIs can involve both chemical modifications and structural variations of the material surfaces.[15] The imprinting approach will allow one to investigate the nature of the probe molecule on the chiral template sites as well as for the surface interactions that allow for the adhesion of the target in different ways. The bisphenol A was chosen as the functional monomer that allowed for an interaction of the chirally printed molecules and the reversibly bound BPA-based MIP because it had a unique chemical nature and the localization of a phenolic hydroxyl group,[16] enhanced the critical transfer of a preferential chiral species from an aqueous to the adsorbing surface layer that involved changes in the chemical nature of the template; second, it also accumulated at the polycarbonate surface of the plastic, where it can exhibit a disruptive interference to an endocrine function such as a growth hormone receptor.[17] This may lead to an understanding of the natural systems and enable the detection or assessment of any undesirable forms in the raw materials or formulation units; moreover, it is important for applications to drug development.

Thalidomide was the drug of interest used in this study. When it was introduced half a century ago, it was used for inhibiting immune and inflammatory responses mostly in pregnant women. In addition, thalidomide caused angiogenesis in the treatment of erythema nodosum leprosum and myelodysplastic syndrome as it affected TNF-α but not the other cytokines.[18] Unfortunately, each mirror image form of the chiral drug had different biological activities, some causing serious toxicity such as those of the (*S*)-thalidomide. As a consequence, the use of the racemic mixture was restricted for many years. Due to the fast bidirectional chiral inversion in physiological conditions and in blood, we have not been able to benefit from the many potential beneficial activities of the (*R*)-thalidomide. The procedure for the production of an MIP was previously reported with the use of a monomeric system that mimicked the binding of thalidomide to DNA,[19] and that sensitive means have now been developed to identify potentially harmful mirror images of thalidomide.[20] The previous studies reported that thalidomide dramatically decreased the glial activation and the beta amyloid neuropathology in a transgenic mouse model that showed symptoms of Alzheimer's disease.[21] Within this work, the deposition of a recognition material on a quartz crystal microbalance was conducted using the imprinted polymer to recognize the racemate and also the individual chiral species. We used a biomimetic surface embedding MIP-sensor layer for the study of surface chemistry and for detailed energetic variations of the polymer surface. Modification to the surface coating of the BPA-bound MIP layer allowed for structural integrity within the chiral imprint of the polymer matrix. This method offers advantages for the formulation to make it possible to predict the processing performance of chirally pharmaceutical compounds, and the mechanism that underlies the different effects of endocrine-disruptive chemicals on the stereochemistry of the biomimetic site. The fine-tune adjustment of an interactive binding site on an MIP can be assessed by a spectroscopic method, and can be verified as a molecular probe for detecting the analytes. The MIP-based QCM used in this study might provide for an easy, rapid, and rugged method for the analysis of chiral pharmaceutical compounds, and may make available a suitable way to study protein interaction *in vivo*.

This article reports the development of a polyurethane layer imprinted with the (*R*)-thalidomide and (*rac*)-thalidomide to serve as the templates for a QCM sensor measurement performed with an enhanced efficient imprint. We carried out the polymerization processes by utilizing synthesized polymer ingredients consisted of *p,p′*-diphenylmethane diisocyanate (DPDI) with phloroglucinol as the cross-linking agent. Also, the experimental conditions that affected the production of a suitable chemical environment of the surface on an Au-coated QCM electrode during the polymerization step were monitored using Attenuated total reflection-Fourier transform infrared spectroscopy (ATR-FTIR). Atomic force microscopy (AFM) was employed as a tool for the characterization of the patterned surfaces of either the racemate or single enantiomer template molecules onto the imprinted polymer layers in comparison to the control polymer. The detection of a signal response was carried out to ensure its concentration dependence on the obtained

MIP layers using a QCM transduction system. Finally, we examined the changes of the adsorption energy from the measured frequency shifts of these analytes on a QCM sensor as well as for the quantitative analysis of specific chiral compounds. The results of changes to the chemical surface environment are also discussed.

EXPERIMENTAL

Chemicals and Materials

(+)-(*R*)-Thalidomide (98.0%) and (±)-(*RS*)-thalidomide (99.0%), *p,p′*-diphenylmethane diisocyanate containing 30% triisocyanate (DPDI), and poly(4-vinylphenol) were from Sigma-Aldrich (Steinheim, Germany); 2,2-bis(4-hydroxyphenyl)-propane (bisphenol A, BPA) was from Merck (Hohenthurm, Germany); and phloroglucinol was from Fluka (Steinheim, Germany). All other solvents were obtained from Labscan Ltd. (Ireland) and were of analytical reagent grade and dried in a molecular sieve before use.

QCM Electrode

To obtain the mass-sensitive devices in this study, two electrode pairs were generated on 10 MHz AT-cut quartz discs with a diameter of 15.5 mm, a thickness of 168 μm, and a resonance frequency of two electrode pairs (each with a diameter of 5 mm) that were generated on the quartz using a screen-printing procedure similar to the one described in a previous report.[22] This dual electrode design with imprinted and nonimprinted polymer layers (NIP) was designed to eliminate any undefined effects that may be caused by temperature fluctuations, conductivity, and viscosity. After screen-printing, the gold was pasted onto the piezoelectric quartz crystal disc by the soft-lithographic method. The electrode structure was burned at 450°C to yield a highly robust gold electrode with good mechanical features and as a result limited any peeling-off effects when exposed to harsh conditions.

Preparation of the Molecularly Imprinted Layers

Materials for imprinting were prepared by polymerizing a monomer solution until it reached the gel point. We first optimized the polymeric composition of the film coatings, and the polymerization of the pre-polymerization reaction was carried out to produce a polyurethane film layer imprinted on a QCM electrode by preparing a mass-sensitive electrode. A mixture of 2.5mg (*R*)-thalidomide or (*rac*)-thalidomide (template), DPDI (15.0 mg), BPA (15.0 mg), phloroglucinol (7.5 mg), and poly(4-vinylphenol) (7.5 mg) was mixed into 1 mL of a porogenic solvent: pure tetrahydrofuran (THF), 50% dimethylformamide (DMF) in THF, or 25% pyridine in THF. The monomer mixtures were pre-polymerized at 70°C for 20 min. The polymerizing solutions were diluted in THF before dropping onto the electrode surface of the quartz discs for further processing. The QCM electrode was then spin-coated at 3000 rpm for 1 h to produce a thin-film layer, and it was hardened overnight at 70°C under nitrogen gas. During template removal, the differences in the FTIR spectra between the MIP-polyurethane-coated quartz before and after washing with 5% acetonitrile/water at room temperature were examined by checking for a lower adsorption peak of the C–O stretching or for no peak at all at 1050 cm^{-1}. The selectivity of the MIP layer can be defined by comparison to a corresponding NIP prepared in an identical manner to the MIP upon polymerization, but omitting the template molecule. The surface morphology and topography of the sensor layer were inspected using the AFM method after the templating process. All AFM images were obtained with a Veeco NanoScope IVa system operating in the contact mode (Veeco Instruments, Plainview NY), with Veeco SNL-10 silicon tips and a spring constant of 40 Nm and an onset pressure that corresponded to a differential signal of 1 V on the photo diode. To obtain an image, the substrate containing the imprint was mounted onto a sample disk and scanned with scan rates in the range of 1–2 Hz at room temperature.

Attenuated Total Reflectance–FTIR Spectroscopy Studies

In this experiment, the study of the polymerizing conditions for the manufacture of the MIP film on a quartz disc was performed by ATR–FTIR measurements. All FTIR spectroscopy measurements of the molecularly imprinted films were carried out on the attenuated total reflection (ATR) cell of a Perkin–Elmer FTIR 2000 system. The ZnSe ATR crystal used had a total of 12 reflections on its surface and used 64 scans at a resolution of 8 cm^{-1} in the range of 600–4000 cm^{-1} and an optical path difference velocity of 0.2 cm s^{-1}. We first optimized the amount of the functional monomer required to produce the MIP film on a QCM electrode by initially preparing a set of templates and monomer mixtures for the polymerization of the film coatings at 70°C in 25% pyridine in THF as the porogen. By varying the mole ratios of template to the functional monomer, their FTIR spectra were determined by providing the observed changes of the absorption bands at 2271 cm^{-1} as a function of time. Thus, it was possible to detect the completion of the reaction between the −NCO and the −OH functional groups of the chemical precursors in the polyurethane reaction mixture that enabled an examination of the fabrication of the imprinted layer that occurred after 40 min. Then, the optimal reaction parameters, including the solvent and the conditions for synthesis wherein the (*R*)-thalidomide enantiomer was used as the template molecule, were determined, in which these polymer films were synthesized with respect to the template with a fixed amount of the pre-polymerized mixture.

Sensor Measurement with QCM

Each measurement using the QCM sensors was performed with a coated electrode in a custom-made measuring cell with a 180 μL volume, cast with polydimethylsiloxane (PDMS), and operated in the stopped-flow mode at a measuring temperature of 25°C. The QCM electrodes were connected to an oscillator circuit that was connected to a frequency counter (Agilent 53131A, CA), which was read out by a custom-made Labview® routine via a GPIB-USB interface. The (*R*)-thalidomide and (*rac*)-thalidomide were dissolved in acetonitrile to obtain an appropriate concentration; then the solution was injected into the flow cell using a Hamilton syringe. A typical measurement cycle consisted of filling the cell with water at 0.35 mL min^{-1} or until the quartz crystal sensor produced a stable response.

RESULTS AND DISCUSSION

Characterization of the Surface Chemistry of the Imprinted Poly(urethane) Sensor Coatings

Scheme 1 illustrates the general procedure for producing the poly(urethane)-imprinted polymer, as well as the nonimprinted

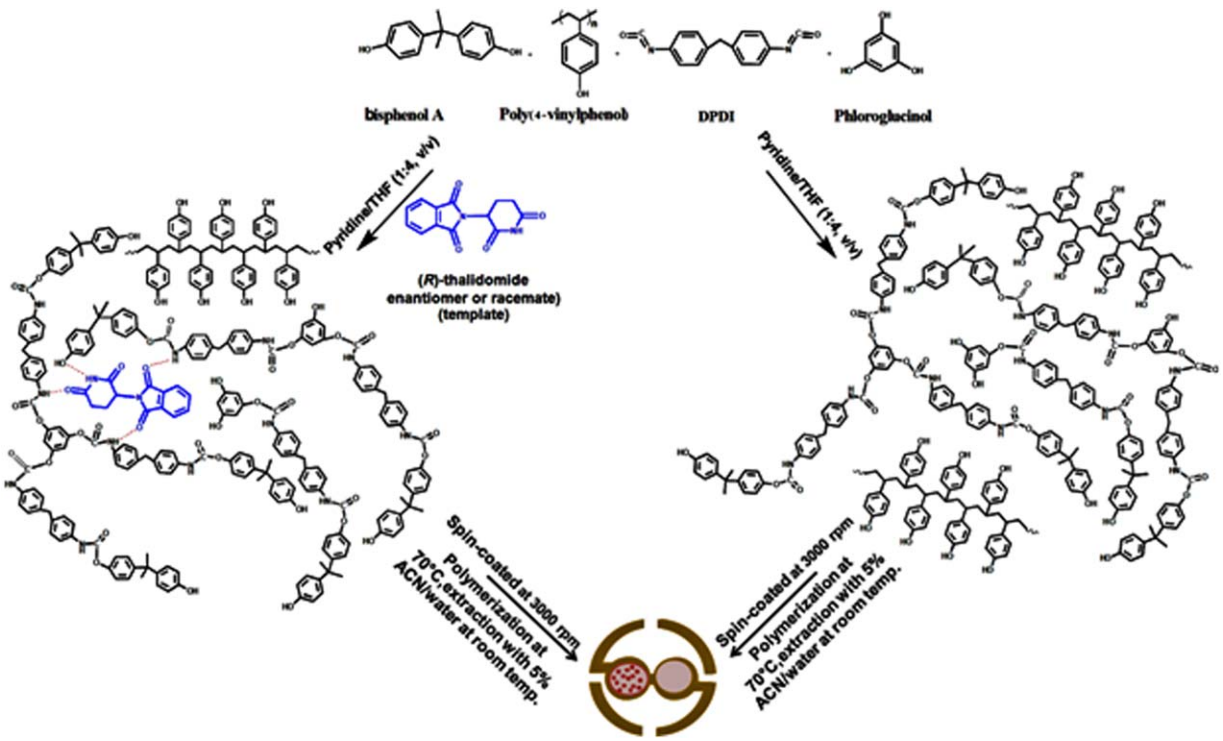

Scheme 1. The illustration of the general procedure in the preparation of poly(urethane)-imprinted polymer and the nonimprinted control polymer on the gold surface of coated quartz disc onto a 10 MHz QCM electrode in this study. [Color figure can be viewed in the online issue, which is available at wileyonlinelibrary.com.]

polymer used as a control, both generated on the gold surface of a coated quartz disc onto a 10 MHz QCM electrode for an efficient template rebinding. After removal of the template, the generation of the optimized template-site was achieved using a cross-linked phloroglucinol polymer to provide robustness for the resultant layer coatings. The study of the surface topography with AFM images showed that a racemic thalidomide–BPA-bound MIP film had been obtained after preparation on the QCM surface and exhibited the structure of a racemic thalidomide template carved into the molecular imprint of the polymers [Figure 1(a)]. The AFM images of the optimized sensor layer were used for characterization of the chemical surface of the poly(urethane)-based MIPs obtained for imprinting the (*R*)-thalidomide and (*rac*)-thalidomide onto the surface of an Au-coated QCM electrode. The imprinted cavities had dimensions of 150–260 nm, with a depth of 80–100 nm into the surrounding of globule polymeric chains that ranged in the submicron size [Figure 1(a)]. The sensor layer showed the part of the surface pattern that was embedded onto the dense packing of the polymer that had the dimension of a hollow by about 560 nm and a depth of 280 nm, in relation to the BPA surface on the thin-film after interaction with the racemic thalidomide that was similar to the NIP control polymer, [Figure 1(c)], to indicate the high nonspecific adsorption on the QCM sensor. In contrast, in the AFM image [Figure 1(b)], the MIP layer coating the (*R*)-thalidomide structure had a depth of about 100 nm into the QCM, where the self-assembled monolayer of the imprint poly(urethane) was coated onto the gold electrode, and the entire enantiomer to enter into the recognition cavity, and then had the appearance of the adapted morphology to a flake-like layer. This was the same for the (*R*)-thalidomide selective NIP [Figure 1(d)], wherein 40 nm holes were generated in the surface layer, which were comparable to the QCM obtained from the NIP. The clear racemic thalidomide-imprint patterns are readily apparent, which demonstrate the tremendous power of this method. The appearance of the self-organized assembled BPA surface with the template can be explained as being the result from the annealing of a thin-film that became swollen in 25% pyridine in THF, that was caused by the hydrophilic and hydrophobic segments, which led to the phase-selective chemistry of the polymeric film. The AFM images demonstrated that the structure and the reorganization of the assembled BPA-surface was associated with the interaction of the template and the MIP to enable the patterned surface of the two mirror image forms of thalidomide during the imprinting process. Evidently, MIP cavities were produced in almost equal amounts for two mirror images of enantiomer for the racemic compound. This may provide evidence for the handedness of the molecules that had been imprinted onto the poly(urethane) film, and could provide an opportunity to resolve the chiral entities of the (*rac*)-thalidomide by a molecular imprinting approach. The fabrication of differently nanopatterned surface of the pure enantiomer of thalidomide and the racemic mixture of thalidomide can be generated by molecular imprinting approach at the surface that had a more defined shape of the drug in the bulk layer that was attributed to the formation of only one form of imprinted cavity. These findings were supported by the AFM of a previous study, which showed that the thalidomide and the

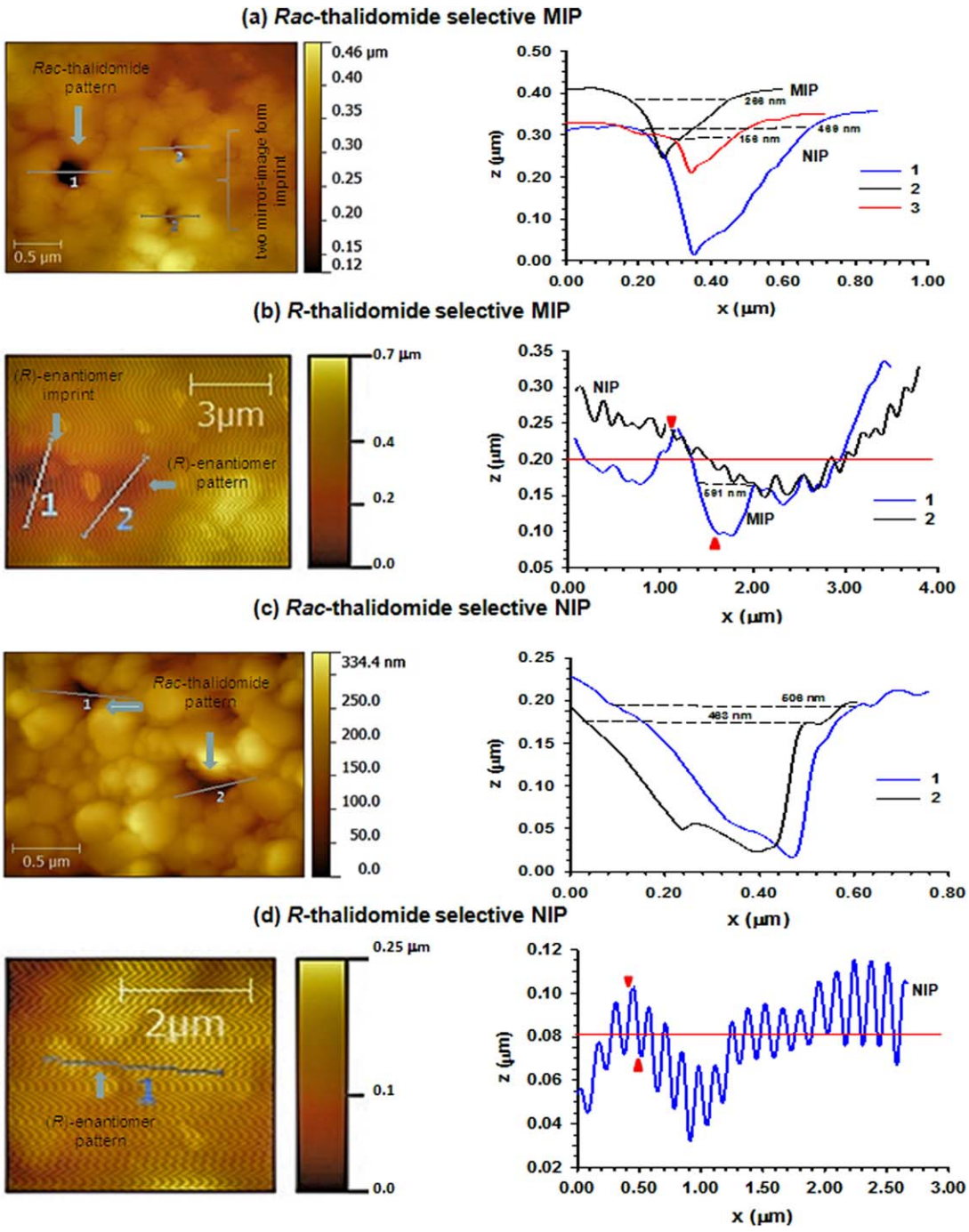

Figure 1. Right: the AFM images of MIP and corresponding NIP consisted of bisphenol A surface were achieved by a spin-coating technique onto a 10 MHz QCM, showing self-organization of the polymer structure and selective patterns of various chirally imprinted molecules in the layered polymer after template removal and exposure of the template. Left: cross-section of the internal structure of the pores. (a) racemic thalidomide-selective MIP, (b) (*R*)-thalidomide–selective MIP, (c) racemic thalidomide-selective NIP, and (d) (*R*)-thalidomide–selective NIP. [Color figure can be viewed in the online issue, which is available at wileyonlinelibrary.com.]

DNA interaction formed a spherical aggregate on the polymer film, with a size of about 2 nm, and was dependent on the thalidomide concentration.[23] The transmission of chirality into a large architecture of biomacromolecule assemblies from molecule–surface interactions and template morphology is usually in the microscale.[24] When considering that the MIPs made for this study mimicked the chiral molecule of the natural surfaces, and could then effectively adsorb the molecules in a favorable arrangements, this could help us to understand the structural relationships for the interaction of proteins and their biological activities. The imprinting efficiency reflected the kinetic effects and its influence on the chiral recognition.[25] The AFM images of the molecular orientation, in addition to surface topography and the organized nanostructures on the film-layers for both

chiral species, should provide us with knowledge of the underlying processes for an efficient imprinting in which further study of QCM sensor will be required to investigate and change the sensor signal.

Description of the Synthesis of the MIP Formulation

In this section, the ability of the functional monomer, that was complementary to the template during the imprinting process and reflected the capacity of the imprint, was evaluated by comparing the variations of the FTIR spectra. The effect of varying the polymerizing components on the pre-polymerization reaction of the polyurethane imprint was examined at a mole ratio of the (*R*)-thalidomide template to the functional monomer of the polyurethane layer coating of (1 : 1–1 : 8) in a mixture of pyridine : THF (1 : 4, v/v). As can be seen in Figure 2, the broad peak at 3410 cm^{-1} could be assigned to a stretching vibration of the O-H groups in the BPA. The peak at the 1720–1740 cm^{-1} region for the aromatic C=C bond was observed in the IR spectra. At a high concentration of the imprinting small molecule in the synthesis, i.e., at 1 : 1 and 1 : 2 template–monomer mole ratios, this resulted in a shift of the thalidomide spectrum peak at 1712–1736 cm^{-1}, and there was a slight change, from 3320 to 3350 cm^{-1}, in the FTIR adsorption peak of the O–H groups of the BPA. This broadening of the thalidomide spectrum was attributed to the hydrogen bond interactions between the hydroxyl groups on the BPA and the imido N–H moieties in the (*R*)-thalidomide structure that were formed in the porogen solvent. There was an increased intensity of the spectrum peaks from 1200 to 1520 cm^{-1}, and it was clearly observed because of the increased rigidity of the cavities that represented the improved functionalities that interacted with the (*R*)-thalidomide structure in the imprinted cavities. We have point evidence now for the recognition mechanism of the MIP using BPA by varying the functional monomers, which had become cross-linked and integrated into the macromolecular networks from 1 : 1 to 1 : 8 template : monomer ratio. The FTIR spectroscopy revealed a skeletal vibration of the aromatic C=C bonds that shifted and broadened, thus confirming that there was probably a π–π interaction between the benzene rings of the (*R*)-thalidomide structure and BPA functional monomer (see Figure 2). At a 1 : 8 mole ratio of template to monomer, the remaining functional monomer BPA appeared with an adsorption peak of the OH group at 3350 cm^{-1}. A lower template : monomer ratio of 1 : 4 exposed the most favorable polar hydroxyl functions that resulted in the necessary observed changes of the absorption bands of the OH---N bond at about 3400 cm^{-1}, which was higher than that for the 1 : 8 ratio. The former case showed a dominant potential hydrogen bonding from an amide carbonyl oxygen atom between 1720 and 1740 cm^{-1}. It seems that the use of the BPA functional monomer promoted the changes in the surface chemistry of the templating enantiomer, to form a high recognition site by a highly rigid receptor. In addition, the changes of the FTIR pattern of the (*R*)-thalidomide as a function of the amounts of BPA could be taken into account to produce the structural dissimilarity eliciting activities of the (*R*)-thalidomide enantiomer.

Furthermore, the effect of the polyurethane on the structure of the coating layers was performed at a 1 : 4 mole ratio of template and monomer, which showed that the 1 : 4 (v/v) pyridine : THF mixture was the most suitable porogen among the other solvents tested, i.e., pure THF and 50% DMF in THF, as it produced the largest changes in the absorption bands at 2271 cm^{-1} (–N=C=O) in the IR spectra (data not shown). This result demonstrated the discrete hydrogen donating/accepting ability for the (*R*)-thalidomide in a solution, which was influenced by the spatial distribution of the (*R*)-thalidomide in the organic solvents and solvent mixtures differently. In a strongly basic solvent, the specific interactions of the solvent with the functional monomer and cross-linker led to weak intermolecular hydrogen bonds between the MIP and (*R*)-thalidomide, even though this was the reason for the high template solubility. In addition, the use of a 1 : 4 (v/v) pyridine : THF mixture produced a spatial distribution of the molecules within the polymeric matrix, while allowing for more changes to produce a better fit to recognize the chirally active pharmaceutical ingredient in this solvent and enhanced the shape and substrate specificity. These results also turned out to facilitate the developing dosage formulation or pharmaceutical processing where a major concern was the association to the dynamic behaviors of (*R*)-thalidomide in the solid state chemistry. Therefore it was important, that the observed phenomenon of the interactions of the (*R*)-thalidomide and the position of the equilibrium provided the best polyurethane layer that was most suitable for the imprinting process, leading to a BPA functional group and carbamate group on the resultant thin-film after removal of the template. It appears that in these cases, the precise control obtained by defining the surface chemistry of the functionalization occurred during the polymerization process.

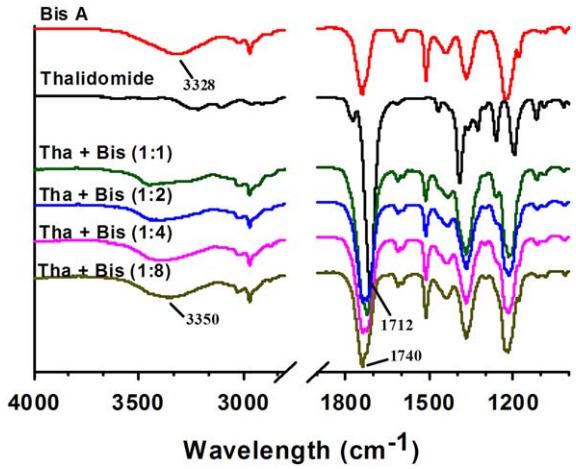

Figure 2. FTIR spectra of the (*R*)-thalidomide, bisphenol A, and the mixture of (*R*)-thalidomide and bisphenol A at different mole ratios. [Color figure can be viewed in the online issue, which is available at wileyonlinelibrary.com.]

Sensor Response

In this technique, the deposition and interaction of the respective sensor layers occurred on a QCM electrode that was excited to oscillate at its fundamental resonance frequency. The increased mass (*m*) resulted in a measurable decrease of the oscillating frequency (*f*) as measured by the QCM technique. For the very thin or quasi-rigid layers, the frequency shift of the

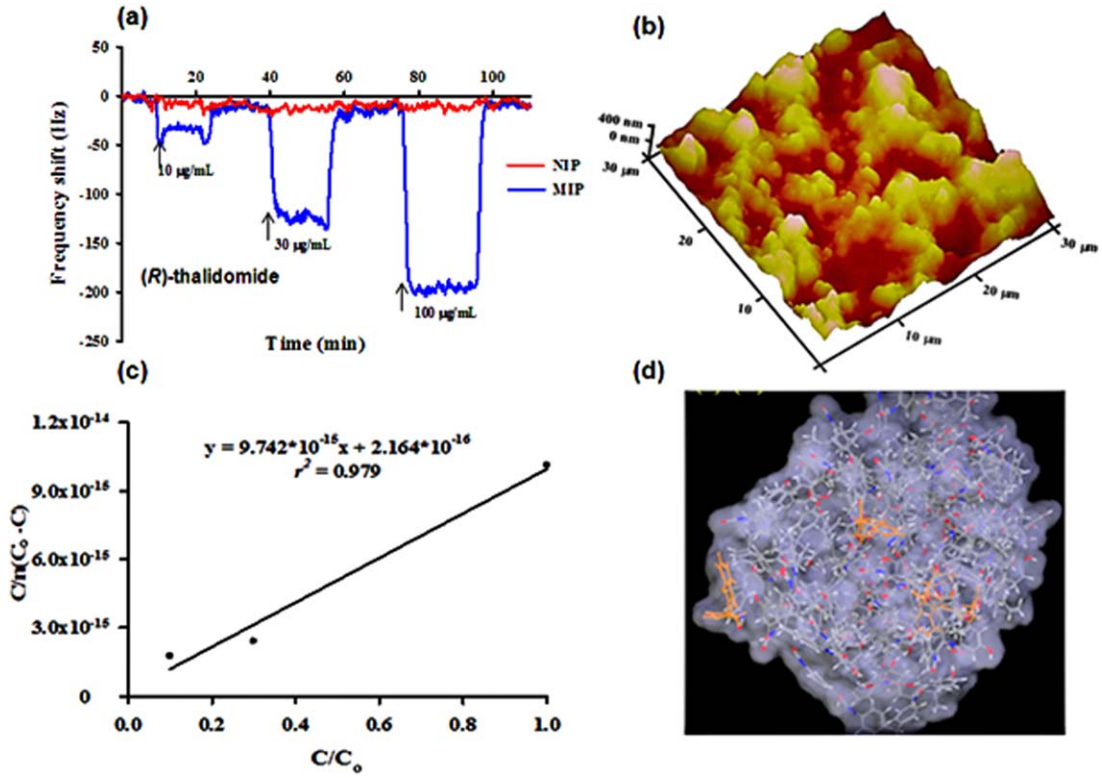

Figure 3. (a) A typical sensor response for the imprinted and nonimprinted polymers illustrating the incorporation of an (*R*)-enantiomer imprint toward the template: the frequency shifts were fast and show a fully reversible adsorption in water at 25°C with a flow rate of 1 mL min^{-1} using a QCM stopped-flow measurement. (b) AFM image of the chemical pattern of the surface sites onto (*R*)-thalidomide-imprinted polyurethane layer coating onto the QCM. (c) The adsorption isotherm of (*R*)-thalidomide onto the respective imprinted layers in water at 25°C. (d) The possible MIP binding site of the (*R*)-thalidomide enantiomer. [Color figure can be viewed in the online issue, which is available at wileyonlinelibrary.com.]

oscillating crystal (Δf) was directly related to the increase in the mass per unit area (Δm) according to the Sauerbrey relationship.[26] Figure 3(a) shows a sensor response of the (*R*)-thalidomide MIP layer that had been coated onto the 10 MHz QCM sensors after exposure to various analyte concentrations as a function of time. When they were exposed to a solution of the (*R*)-thalidomide template at a concentration of 100 μg mL^{-1}, this led to a net frequency effect or the difference in a frequency shift response between the MIP and the reference of up to 200 Hz. The reversible rebinding of (*R*)-thalidomide appeared, as well as the homogeneity of the surface chemistry, which was proven by the AFM images [Figure 3(b)], thus indicated a host–guest binding by this MIP system. The discrimination based on the measured QCM frequency responses for each of the MIPs was evident and a distinct trend was observed. The increase in the overall net effect was as high as 200 Hz on the QCM through the layer imprinted with the (*R*)-thalidomide, and this provided a substantial amount of sensitivity while a substantially lower analyte concentration for any nonspecific adsorption was achieved.

We found that it was of considerable importance that [Figure 4(a,b)] using the present measuring conditions that the racemic thalidomide-imprinted polymers showed a positive QCM frequency shift when they were exposed to 10 and 100 μg mL^{-1} (*rac*)-thalidomide. As seen in Figure 4(a), the artificial materials produced a slightly positive sensor that changed to 40 Hz upon exposure to the 10 μg mL^{-1} of the racemic thalidomide, while the frequency shift of the nonspecific binding on the NIP channel was about 10 Hz lower than for the imprinted layers. In contrast, there were substantial higher frequency effects in the layer imprinted with the (*rac*)-thalidomide, when exposed to a pair of mirror image forms that were formed at a concentration of 100 μg mL^{-1} and produced a positive signal that changed by between 300 and 350 Hz that was twofold higher when compared to the NIP layer. The high concentration of the (*rac*)-thalidomide led to frequency shift signals that were superior in the MIP-based sensor toward the corresponding template in a water medium, meaning that the presence of the BPA-binding groups not only brought the observed changes in the sensor signal but also achieved chiral recognition properties. With a unique internal pore morphology of the polymeric structures, steric arrangement of binding site interactions in the molecular imprinting of poly(urethane)-coated QCM have been proven, that significantly influence the control surfaces, while specifically orientating the enantiomer inside the corresponding cavity. It can be concluded that a highly specific recognition on the active material on the surface was reproducible for the chiral molecule.

Furthermore, it appeared that the normal baseline of an (*R*)-thalidomide MIP-based sensor changed from 12 to 20 Hz upon the addition of 10 and 100 μg mL^{-1} of a single thalidomide

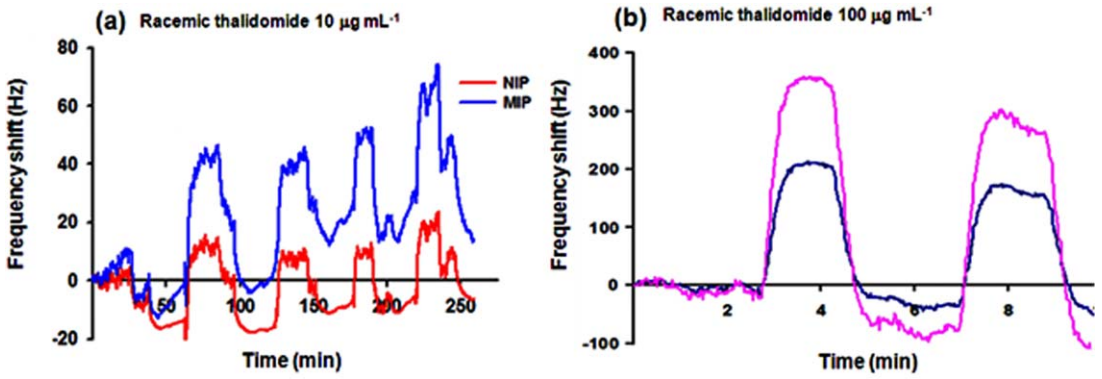

Figure 4. The positive frequency shifts of the racemic thalidomide-imprinted polymer and the nonimprinted polymer coating onto the 10 MHz QCM exposed to two different concentrations of racemic thalidomide at (a) 10 μg mL^{-1} (flow rate of 0.35 mL min^{-1}) and (b) 100 μg mL^{-1} (flow rate of 2.45 mL min^{-1}) at room temperature. [Color figure can be viewed in the online issue, which is available at wileyonlinelibrary.com.]

enantiomer solution in water, respectively, and it actually presented an excellent sensor effect for the (*R*)-thalidomide. The frequency shift of the NIP-based polyurethane sensor turned out to be as low as 15 Hz due to (*R*)-thalidomide. This was in contrast to the (*rac*)-thalidomide-imprinted poly(urethane) where the sensor signal changed from 20 to 40 Hz upon the addition of 50 and 100 μg mL^{-1} racemic thalidomide, [Figure 5(a)]. An increase in the QCM signal responses for the respective NIPs was exhibited between the two chiral templating compounds. This can be attributed to the differences in interactions toward the pure form and a racemic mixture in the chiral compounds and the functional groups in the layered polymeric materials, which showed a higher nonspecific adsorption of the racemic compound than to the single enantiomer. Hence, it is likely that the more weakly bound species may lead to stronger nonspecific adsorptions due to the very restricted motion of a chiral racemic compound within the imprinted cavity.[27] In addition, different positive and negative frequency shifts were shown after the alterations by the mechanical whisking of the different flow rates of the medium. Notably, they can oscillate together with the sensor layer on the device, leading to a mass response, i.e., a negative frequency shift. These results indicated that the effect of the molecular shape in a bulk solution was important, and was reflected in the molecule environment, that was presented in the AFM image. It is possible that the assessment of its surface energetic properties can be obtained from the commercially available racemate thalidomide using this technique.[28,29] Our findings have clearly indicated that the bisphenol A-assembled (*rac*)-thalidomide in a putatively selective matrix of the polymer structure had an anisotropic surface.

Furthermore, we related the phenomenon of the sensor response to the (*rac*)-thalidomide by the respective sensor and its effects on the properties of the surface functionality. With regard to the above-mentioned results, the detailed surface energetics of the chiral species from the measured sensor signal was determined and a hydroxyl group from the bisphenol A in an MIP was identified, thus allowing for the template to be rebound onto the QCM sensor.[30] Figure 5(b) illustrates the plot of the frequency shift vs. the concentration of the solutions of the racemic thalidomide in water at 25°C. The racemic thalidomide imprint onto the QCM sensor ranged from 1 to 100 μg mL^{-1}, which showed that the characteristics of the sensor signal were the same as that of the single (*R*)-enantiomer imprint exposed to the analyte, and reached the chirally selective sites. The result exhibited positive frequency shift that were turned into the expected negative ones and gave rise to frequency shifts of from −40 to −80 Hz, as the concentrations increased from 100 to 200 μg mL^{-1}, respectively. The MIPs also facilitated the observed change in a substantially different sensor response at concentrations of the racemic compound above 100 μg mL^{-1} [Figure 5(b)]. The racemic thalidomide-imprinted layer also led the sensor response to the analyte species into the bulk selective layer at lower concentrations, and would appear to be recognized by the selective pattern of the racemic thalidomide. At high concentrations of (*rac*)-thalidomide in acetonitrile there was an induced dynamic process to the assembled BPA in the MIP, albeit with several weak intermolecular forces such as hydrogen-bonded assemblies that stabilized the template–bisphenol A interaction at the surface of the polymer coated onto gold electrode. Thus, difference between the molecular structures of pattern originated from the difference in their intermolecular interactions between H-bond interactions. It is feasible that as a consequence of the organization process that occurred between the templating entities and the functional groups as shown by the sensor response patterns, on the sensor measurements.[31] In this case, the racemate compound presented a high level of surface heterogeneity in the MIP layer to serve as an alternative means for a molecular-replacement study when the crystal of a given protein was only produced with difficulty.[32] Molecular monitoring of influences induced by the environment formed altered internal pores of the self-assembled MIP-template within the sensor layer and resulted in a reversible signal for the chirally imprinted compounds that was dependent on the chemical functionalization and interactions in the solvent, and this agreed with previous imprinting methodologies.[13,15,33] In comparison to the nonspecific effects on the reference electrode, the frequency shift responses increased as a function of the analyte concentrations with almost the same slope, to indicate that the different isomers of the racemic thalidomide were not being resolved. Incorporation into the specific

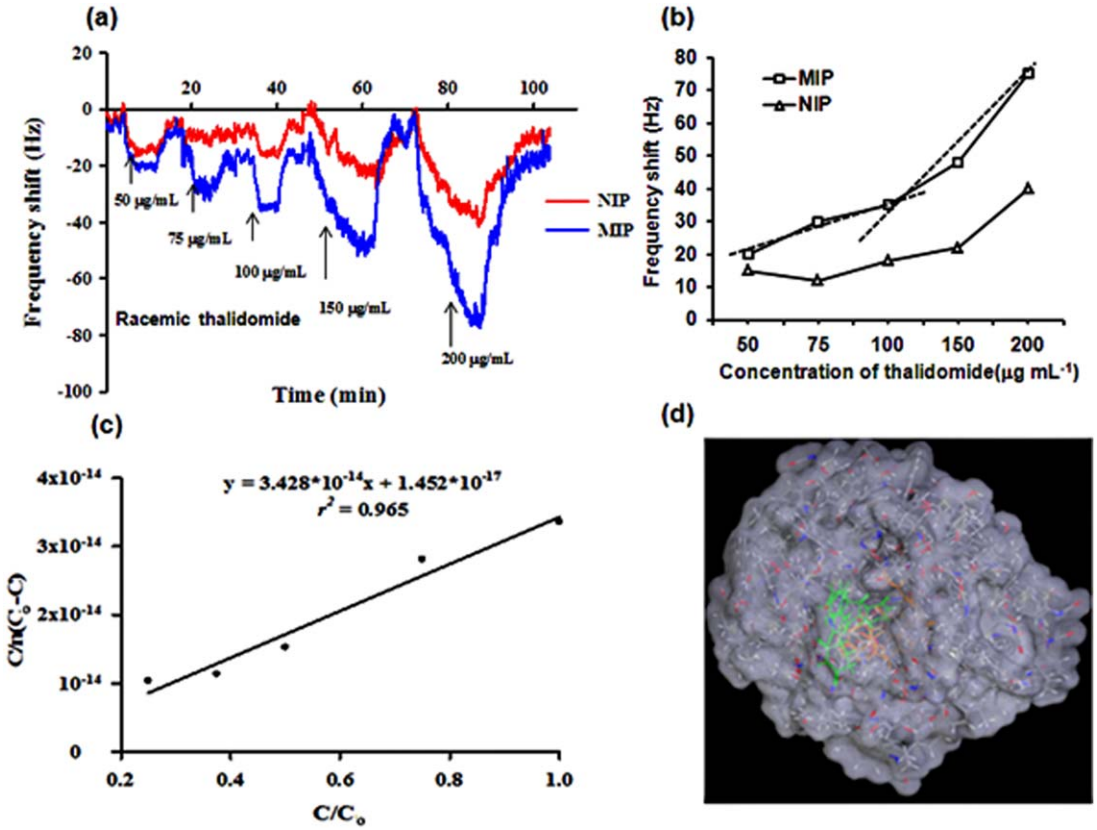

Figure 5. (a) A 10-MHz QCM response of a racemic thalidomide molecularly imprinted and a nonimprinted polyurethane onto the QCM. (b) The plot of oscillating frequency shift of the racemic thalidomide as a function of the racemic thalidomide concentrations in water at 25°C. (c) The adsorption isotherm of the racemic thalidomide onto the respective imprinted layers in water at 25°C. (d) The interaction of (*R*)-thalidomide (orange) and (*S*)-thalidomide (green) with the polymer surface of racemic thalidomide imprinted cavities. [Color figure can be viewed in the online issue, which is available at wileyonlinelibrary.com.]

imprinted cavities on the self-assembled monolayer that had high free energy sites on the film coating could interact preferentially with the individual thalidomide and the racemic mixture of thalidomide in the water, into well-defined structures on the surface of the device, as shown by the signal of the sensor. In contrast interaction with low free energy sites was for the adsorbed molecules that provided information concerning the dynamics and surface properties of these different chiral species derived from a comparison of the mass-sensitive detection in various samples. By contrast, the binding of the racemate analyte reached only one half of the racemic thalidomide-selective NIP in the reference channel over a 60-min period. As the prepared polymer nanostructures of the polymeric layer used to coat the QCM may pursue the application for detecting the formation of trace amounts of the unwanted molecular form. The stabilization times after each addition were different, depending on the chiral analyte species, for example, approximately 30 min was suitable for the racemic mixture and 25 min was suitable for the pure enantiomer. These times were governed by the diffusion pathway and by the specific interaction of the assembled BPA to the templates in the MIP cavities. Recent efforts have been made to understand the molecular structure of the BPA on the nanomaterials such as graphene, which provided the electronic properties and the high conductivity.[34] The dynamics and organization of the molecules in the polymer system needed to be characterized according to their binding affinity and their interactions by several methods for the assessment of their surface energetics.[35] This produced an additional number of interactions between the analyte by the chiral recognition sites. Another important finding was that there was an observed difference in the sensor effect, which demonstrated that the imprinted polymer layer had special adsorption properties due to the nonspecific binding on the devices that could be attributed to the mobility effect on polymer coatings that have a non-Sauerbrey behavior. Thus, these surface imprints with self-organized recognition sites could detect and evaluate molecular chirality. Taken together with the FTIR spectra, the MIP-based QCM confirmed the presence of different forms of thalidomide that had different biological activities under the same conditions. This effect was attributed to the existence of water in the environment, as this favored binding by the hydrophobic and van der Waal's forces to the chiral species of the API.[36]

Functional Structure Determined from QCM

With QCM sensor measurement, the observations above demonstrated that the two isomers of (*rac*)-thalidomide fit well into the corresponding MIP cavities because of the higher surface contact of the surrounding cross-linked chains. In addition, the

Table I. Surface Energy Data and Binding Parameter of the Imprinted Polymer Thin-Layers on the QCM Measurements

Compound	Energy of binding site (mJ m^{-2})	K_a, binding affinity (mM^{-1})	Δm_{max}, maximum binding for saturation (nmol)	n_m, number of adsorbed molecule
(*R*)-Thalidomide	0.0322	9.98	1.30	2.92×10^{13}
(*RS*)-Thalidomide	0.0654	1.90	0.76	1.0×10^{14}

Note that the depth of layer coating at 400 nm and the area of surface coating was 0.196 μm as determined on AFM images.

ability of the racemic thalidomide MIP-based QCM to measure the different forms of thalidomide was dependent on the parameters of the environmental solvent and the concentrations of the thalidomide isomers that effected changes on the sensor signal. This was also realized by the equal extent of the variations in the surface chemistry of the binding site on either of the thalidomide enantiomers that were complementary to their functionalities. It was attributed to the defined binding-site interactions in the imprinted cavities, together with the nanopatterned surface that facilitated the discrimination of different structural motifs of the chiral species through a biomimetic surface.

Furthermore, the newly developed method permitted the characterization of the chiral compounds, and a detailed analysis of the surface interaction energy would allow us to address the tracking conformation dynamics for the respective molecules that interacted with the physical conditions of the surface. The utilization of quantum mechanical control of small aggregates is well known as it was this that established the chirality on the macromolecular assemblies, e.g., DNA.[37] For the physical adsorption phenomena, the Brunauer–Emmet–Teller (BET) model was suitable to describe the multiple site adsorption.[38] In Figure 5(c), a BET isotherm for the (*rac*)-thalidomide was bound onto the respective imprinted layers that provided for the observable difference between the numbers of binding sites and the binding affinity value, K_a of the two imprints with a highly satisfactory correlation coefficient ($R^2 > 0.96$) of the data.[39] The surface energy data were calculated using the frequency response for both the analytes.[40] The number of adsorbed molecules, n_m value, was obtained from the intercept of the slope. The calculated results are summarized in Table I. The calculations on the adsorbed (*R*)-thalidomide differed by less than threefold to that of the racemic mixture on a racemic layer; in addition, the calculated surface energy of the (*rac*)-thalidomide was twice larger than the (*R*)-enantiomer of thalidomide. The BET plot that resulted from those imprinted materials provided for the adsorbed analytes on the sensor layer. An affinity for binding (K_a) of the (*R*)-thalidomide was fivefold higher in comparison to the K_a value of the racemic thalidomide. In this case, the obtained polyurethane cross-link was devised to change the surface properties toward the binding affinity of (*R*)-thalidomide in an (*R*)-thalidomide MIP with high specificity. The surface chemistry of the MIPs yielded different binding energies by about twofold. It was true that both the volume and surface area of the pair of enantiomers of thalidomide were much larger than in the pure form of the enantiomer, but there was a larger adsorption energy toward the racemic thalidomide compared with that of the pure enantiomer. This, perhaps, was necessarily the case as the intermolecular packing of the (*rac*)-thalidomide containing equal amounts of (*R*)- and (*S*)-isomers, that were assembled at the entrance to the accessible site in the polymeric structure, and also the different distance of binding group interactions and such chiral centers with respect to the pure form of thalidomide. It also seemed that the number of thalidomide enantiomers bound on the patterned materials can induce the chiral compound to become more complementary, which was dependent on the correct choice of the chemical precursor in the MIP. This approach was anticipated to span the range of the chiral enantiomer analyte: if we generated an (*S*)-form imprint to test the pure (*S*)-thalidomide, this might cause side-effects that were related to the chemical nature and the polymer precursor, to only form a favorably resolution structure. The alternative method, which is the biological monitoring based on a biomarker, can be used to assess the potential toxicity of the pure (*S*)-thalidomide that would cause toxicity as previously reported.[41] There was a different effect in the biological system for target recognition because of the variation in the binding modes of the thalidomide enantiomer at the target site.

The BPA that appeared at the surface coating of the sensor should be responsible for the stereospecific interaction that was induced by the thalidomide enantiomer species. There was no similarity between the selective pattern for both the pure single thalidomide and the (*rac*)-thalidomide after the polymerization on a QCM electrode. A model of the possible binding site of the selective sensors obtained from the data of AFM in conjunction with FTIR spectroscopy, as shown in Figure 6(A). The fact that the binding affinity and substrate specificity for both MIPs are superior toward the corresponding template in water provides evidence for the existence of the structure and thermodynamic behaviors from the BPA-active surface of the polymer surrounding (*R*)-enantiomer and its corresponding racemic compound due to the contributions to the observed changes in the chiral recognition properties. This involves complementary hydrogen-bonding sites formed between both templates may be that the BPA used are about the same stoichiometric ratio for a compound of one chiral site on molecular recognition by imprinted polymer cavities and we anticipate that the racemic mixture of thalidomide showed hydrogen-bonded dimers upon the imprinting process. The macroscopic level of the nanosized patterned surface of either the racemic or the pure form of the (*R*)-thalidomide showed a marked difference of the morphology of the template adapted cavity. In addition, the construction of the MIP-based QCM sensor had the anisotropic surface properties with interactive functional groups was shown to detect the properties of the chemical surface and to distinguish the

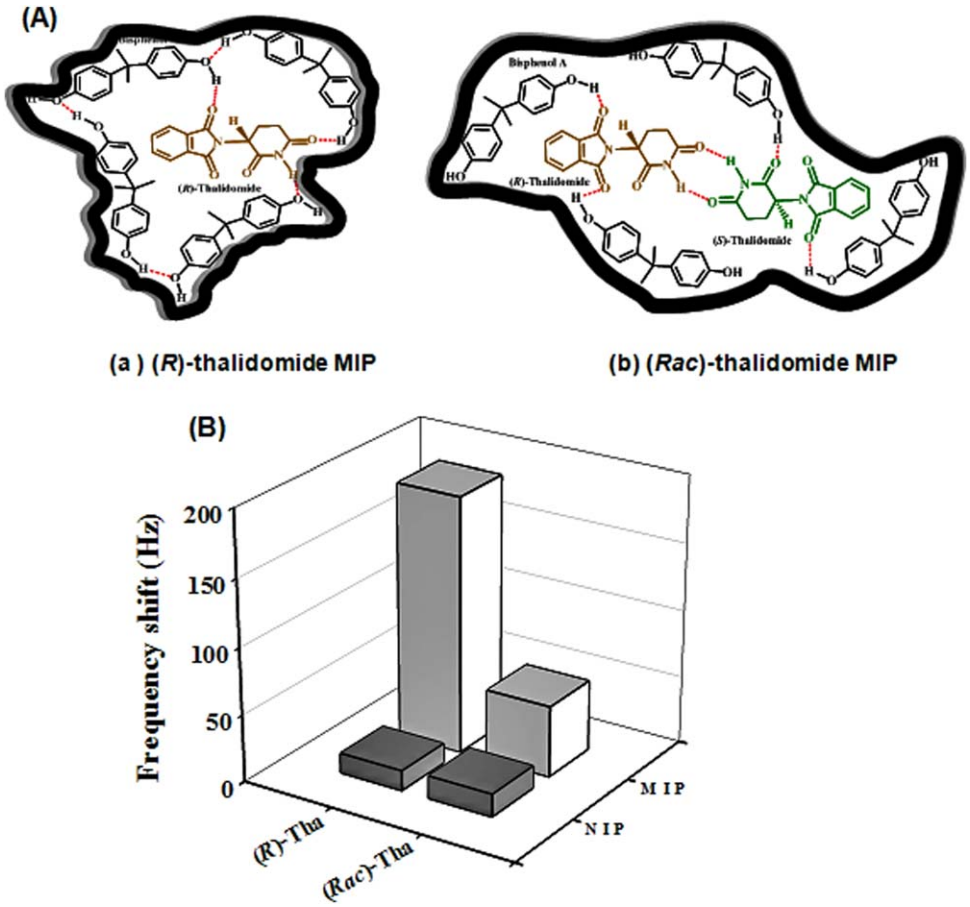

Figure 6. (A) A model for a BPA-based biomimetic functional surface on (a) (*R*)-thalidomide-selective polyurethane sensor and (b) racemic thalidomide-selective polyurethane sensor. (B) Selectivity of the MIP layers coated onto the QCM sensors, which were templated with (*R*)-thalidomide and racemic thalidomide, toward these two analytes. [Color figure can be viewed in the online issue, which is available at wileyonlinelibrary.com.]

energetics of the surface of the different chiral forms of thalidomide. Therefore, differences of the effects indicated the imprinting with the BPA as a functional monomer, favor the adsorption of the thalidomide enantiomers, because of a high level of noncovalent association with the chiral therapeutic molecules inside the imprinted cavities. Clearly, the energy required to reorganize the binding group into a suitable conformation in the presence of strong donor or solvents. From the AFM method, the estimated surface area of the (*rac*)-thalidomide and the (*R*)-thalidomide differed by about one order of magnitude from the estimated number of available imprint sites on a specific area of the QCM. There were a comparable number of imprinted sites for both methods (Table I). At an enantiomer concentration of 100 μg mL^{-1}, n_m, the number of each of the enantiomers for both the (*R*)-thalidomide and the racemic thalidomide that were adsorbed on to the MIP layer differed by being about fivefold, higher for the racemic compound. Furthermore, the spatial distribution of the individual enantiomer cavities and the racemic mixture cavities of thalidomide for their surface energetic properties that were determined through QCM, using the probes partial vapor pressure extrapolated to finite concentration conditions such that a much greater number of such sites could be probed.[42] The numerical determination of the distribution of energy for these chiral enantiomer molecules, showed that the regression coefficient, R^2, was higher than 0.980 for the (*R*)-thalidomide. In addition, the number of calculated binding sites indicated that the functionalities and additional factors (solvent) on the surface properties remarkably affected the recognition selectivity within the chirally template layer.[43] In Table II, the sensor surface had a reduced binding affinity by the MIP compared with the (*R*)-thalidomide–imprinted layer that exhibited a higher value of the monolayer volume V_m of up to 4.5-fold, with two-time differences in *C* (constant) as determined by the shape of the isotherm. Taken together with the AFM studies this indicated that the aforementioned surface energetic properties provided an insight into the chemical information at the level of the pure enantiomer and the racemate.

The recognition system was generated by this approach resulted in the geometrical fitting in the imprint together with an excellent selectivity of the BPA functional monomer in the selective layer. Figure 6B depicts the frequency shifts for both target analytes on the mass-sensitive sensor measurements. The (*R*)-thalidomide, when exposed to these polyurethane layer environments, produced a higher frequency shift than the corresponding NIP control polymer by an astonishing factor of 10. This effect indicated that the adsorbed chiral entities on the

Table II. Parameter for Functional Structure Determined from QCM

Compound	Mass response (Hz)	V_m (cm^3)	C	Surface area adsorbed [a] (μm^2)	Imprints[a]
(*R*)-Thalidomide	−200	7.17×10^3	4.34×10^5	4.57	2.83×10^5
(*RS*)-Thalidomide	−80	1.53×10^4	8.58×10^5	13.7	7.85×10^5

[a] As determined on AFM images.

sensor surfaces could impart a higher order of specificity for the subsequent enantiomer adsorption of the former. A consequence of this effect is that the chemical surface properties of the nanosized cavities with specifically oriented functionalities are obviously able to assemble chiral enantiomer species. It is clearly evident that the sensor effect of the (*rac*)-thalidomide on the imprinted layer relative to the reference sensor was fourfold higher for the (*rac*)-thalidomide than that of the (*R*)-thalidomide, and indicated that the interaction was mainly determined by the amount of one of the two enantiomers present in the (*rac*)-thalidomide at the same initial concentration. This fact emphasizes how important to take the nature of thalidomide enantiomer and racemic compound into account in the prediction of the precise structure and thermodynamic properties associated with the recognition process of the receptors, e.g., a human hormone receptor-selecting specific antibody. A slightly different molecule or undesired enantiomer where steric or spatial distribution caused by endocrine disrupting agent having an inhibitory effect, or an enhanced reaction on molecular recognition by the growth hormone receptors; if the ability is proven to exchange components/recognition groups, so the entities become displaced and away from the active chiral site, hence changes of biological process or modified function of biological system. In addition, the molecular modeling studies and the site expressed differences of the BPA deposited on the surface of the coating layer on the QCM electrode were carried out using HyperChem 7.5 (Gainesville, FL). The Amber MM method, at the H/3–21G* level, was used and showed remarkable differences in three-dimensional structure of the imprinted polymers, as shown in Figures 3(d) and 5(d). It was of great interest to try to understand the underlying mechanism for controlling the stereochemistry in the endocrine disruptors such as BPA to the biological system. The binding of the drug involves H-bonding between the protein–ligand complex, and displays the intermolecular H-bond interactions at the imide of the phthalimide ring of thalidomide in enantiomer and racemic compound. The main difference between these forms of thalidomide is the possibility of differences of interfacial interactions between the −NH and the carboxylic oxygens of the protein and the glutarimido NH and the arrangement of the carboxyl groups at the binding sites on the resultant biomimetic receptor, that perhaps represent the interaction of a hydroxyl group on BPA molecules in the polymer may disturb the binding events. The phthalimide ring may induce an enhanced hydrophobicity, as well as the aromatic hydrophobic interactions. Structural dynamics governs the chirally pharmaceutical binding domains to their receptors in the presence of the BPA-based biomimetic surface. The comparison of the chemical surface properties of the different forms of the chiral drugs has helped to understand the mechanism of the stereochemistry that controls the thalidomide-dependent cellular cytotoxicity *in vivo*. This was thought to be associated with the free energy differences for the existence of endocrine disrupter, BPA, present on the surface of the biomimetic receptor. The difference in the energy of the binding site of the oligomeric membrane receptor and the orientation of the molecules at surfaces have been investigated in a previous study.[44] Collectively, the equilibrium for binding, that followed the time at which the matrix was brought into contact, was related to the actual binding kinetics between the chiral therapeutics and the recognition material. Incorporating these observations with the previously mentioned report, we proposed that the reactions involved in the binding to the same MIP attached to the QCM electrode via two binding processes are: first, there are differences in the stereospecific interactions of both the chiral entities; and second, the effect of the presence of the highly functionalized materials whose defined specific recognition site was inside the coated layer on the QCM. The kinetic rate for thalidomide enantiomers binding to the racemic imprint was rather small because high template concentration was required, there was intricate biological process of adjusting concentrations that in the cell optimal solutions are more easily found. The chiral recognition characteristics of such MIPs were, moreover, indicative of somewhat counterintuitive behavior. Our current data show the structure of selective pattern, and then had the appearance of the adapted morphology, dependent on surface free energy was associated with the adsorbed chiral forms of thalidomide at the surface. Thus, the interaction of thalidomide enantiomer and racemate with the synthetic-estrogen BPA of the layer-coated QCM can determine the efficiency of the biomimetic receptor, in turn, can be used for tracking an event that cell-surface receptor proteins influence biological process and diseases.

Analytical Applications

Under the optimized concentrations, the sensor response was linearly proportional to the concentration of the (*rac*)-thalidomide in the range of 10.0–200.0 μg mL^{-1} and 10.0–100.0 μg mL^{-1} for the (*R*)-thalidomide. The resulting sensors can therefore be used for measuring the maximum drug concentration of the (*rac*)-thalidomide up to 200 ppm. The linear regression equation was expressed as $0.35C$ μg $mL^{-1} + 1.17$ ($R^2 = 0.995$) for the (*rac*)-thalidomide and 1.84 μg $mL^{-1} + 23.95$ ($R^2 = 0.940$) for the (*R*)-thalidomide. For the (*rac*)-thalidomide, the limit of detection (*3S/N*) was estimated to be 0.13 μg mL^{-1}, whereas the limit for detection of the (*R*)-thalidomide was 0.10 μg mL^{-1}, hence, both sensors operate in a concentration range

that was lower than the signal to noise ratio of the sensor response by a factor of 10. The relative standard deviation (RSD) was 2.5%, and this showed a good reproducibility for both the analytes. For the selectivity of the MIP-based QCM sensor, the two different layers showed different sensor responses to the individual enantiomer and the (*rac*)-thalidomide, and they also had different sensor characteristics, which enabled them to be identified qualitatively. However, the qualitative data cannot be achieved by a single sensor but requires an array of sensors.

Moreover, the results as mentioned above indicated that the approach based on the usage of the MIP-based QCM sensor provided the potential means for determination of the dynamic properties on the coating layers that can bind to the corresponding template. The surface energies and chemical information that one can obtain from the creation of an image within the assemblies of the intact monomer-template involving a label-free technique. The on-line measurements of the QCM sensor provided more advantages to the measurements of the sensor responses than those obtained from the media interface of a continuous liquid flow system. The imprinting efficiency reflected the kinetic effects and its influence on the rebinding and signal response of the QCM. The functional material of this MIP system resulted in more efficient for detecting of different chiral species of thalidomide which is a superior method to the previous methods. Since the modulation of the nanopatterned surface of the polymeric layer resulted in a less compact density of the macromolecular chains in MIPs and led to the partial or the full assembly of only one mirror isomer of thalidomide fit well into the respective imprinted cavity after the polymerization process. A sensitive layer based on the MIP-poly(urethane) also allows for it to be used to model the surface energies by evaluating the interactions of the probing molecules oriented on such a surface, as they reflected their surface chemical environment, thus providing additional information of the surface energetics upon molecular recognition. As for the importance of the molecular structure and packing on the imprinted polymer that coated the QCM electrode this can be examined by direct measurements of the discriminating forces. Thus, the imprinted polymer-based QCM is a highly promising approach that has turned out to facilitate its application in drug development.

CONCLUSIONS

In this study, we have described developments in the determination of the properties of chemical surfaces associated with (*rac*)-thalidomide and (*R*)-enantiomer using a molecularly imprinted poly(urethane) polymer that consisted of the synthetic-estrogen bisphenol A that facilitated the localized adhesion of the assembled enantiomers, that were accompanied by structural changes of the polymer architecture. By optimizing porogen solvent, concentration of functional monomer, and reaction time, the synthesized reaction of poly(urethane layer) were prepared in the presence of (*rac*)-thalidomide and (*R*)-enantiomer as the templates on the QCM. Evidently, the generation of the coating layer consisted of forming a phloroglucinol cross-linking matrix covering an Au-coated QCM electrode, at 70°C in 25% pyridine in THF as the porogen. The removal of the template by 5% acetonitrile/water at room temperature resulted in significant changes to the internal pore morphologies and produced different nanosized patterned surfaces for the ability to recognize and respond to the chemical nature and stereochemistry of the template. Both the FTIR spectra and the AFM images readily produced clear evidence for the generation of the selective pattern and revealed different three-dimensional orientation of a thalidomide enantiomer compared to that obtained from a racemic mixture on the polymer structure. The current study has provided an insight into the molecular orientation that requires interactions on the location of the orientation molecules of the racemate that contains two mirror image forms in the imprinted sites. With the results obtained, the imprinted polymer layer precisely manipulated a spatial arrangement of the structure that mimicked the enantiomerically pure form and the racemic compound of thalidomide was regulated by the surface chemistry. This may be the fact that due to the presence of BPA which altered the binding energy of the surface and induced the generation of a better defined site of the enantiomer within the bulk layer. The constructing of these chiral sites relied on a molecular probe, and this turned out to provide information concerning the dynamics and surface properties of these different chiral species of thalidomide in their existence in a solvent environment. Furthermore, the nanopatterned surface of a chiral drug template that was achieved by this imprinting polymer approach may provide valuable information with respect to estimating the qualitative magnitude of the raw materials; the manufacturing process was capable of producing or formulation of a chiral drug; the predictability of biological controls; and appropriate target specific conditions. It was of interest, that this method supported the view of the binding of either the (*R*)-thalidomide enantiomer or the racemate to a protein or other growth hormone receptor providing an enhanced understanding of the specific binding and molecular recognition. Therefore, the energetic advantage of this MIP system provided us with a real-time mass-sensitive detection, and a rapid and reversible binding suitable for the quantitative analysis of these analytes, with a high potential for use in drug development.

ACKNOWLEDGMENTS

We greatly appreciate financial support from: the Royal Golden Jubilee Ph.D. Program (Grant No. PHD/0027/2550); the Higher Education Research Promotion and National Research University Project of Thailand (NRU), Office of the Higher Education Commission; the Nanotechnology Center (NANOTEC), NSTDA, Ministry of Science and Technology, Thailand, through its program of Center of Excellence Network; the Drug Delivery System Excellence Center at Prince of Songkla University, Thailand; and ASEA-UNINET (Austria). The authors would like to thank Dr. Brian Hodgson for assistance with the English.

REFERENCES

1. Vlatakis, G.; Andersson, L. I.; Müller, R.; Mosbach, K. *Nature* **1993**, *361*, 645.
2. Mosbach, K.; Ramström, O. *Biotechnology* **1996**, *14*, 163.

3. Wattanakit, C.; Côme, Y. B. S.; Lapeyre, V.; Bopp, P. A.; Heim, M.; Yadnum, S.; Nokbin, S.; Warakulwit, C.; Limtrakul, J.; Kuhn, A. *Nat. Commun.* **2014**, *5*, 3325.
4. Wulff, G.; Sarhan, A. *Angew. Chem.* **1972**, *84*, 364.
5. Rathbone, D. L. *Adv. Drug Del. Rev.* **2005**, *57*, 1854.
6. Schirhagl, R. *Anal. Chem.* **2014**, *86*, 250.
7. Suedee, R.; Srichana, T.; Martin, G. P. *J. Control. Rel.* **2000**, *66*, 135.
8. Turner, N. W.; Jeans, C. W.; Brain, K. R.; Allender, C. J.; Hlady, V.; Britt, D. W. *Biotechnol. Prog.* **2006**, *22*, 1474.
9. Orozco, J.; Cortés, A.; Cheng, G.; Sattayasamitsathit, S.; Gao, W.; Feng, X.; Shen, Y.; Wang, J. *Am. Chem. Soc.* **2013**, *135*, 5336.
10. Mosbach, K. *Anal. Chim. Acta* **2001**, *435*, 3.
11. Dickert, F.; Hayden, O.; Bindeus, R.; Mann, K-J.; Blass, D.; Waigmann, E. *Anal. Bioanal. Chem.* **2004**, *378*, 1929.
12. Hayden, O.; Haderspöck, C.; Krassnig, S.; Chen, X.; Dickert, F. L. *Analyst* **2006**, *131*, 1044.
13. Lieberzeit, P. A.; Dickert, F. L. *Anal. Bioanal. Chem.* **2008**, *391*, 1629.
14. Ye, L.; Mosbach, K. *Chem. Mater.* **2008**, *20*, 859.
15. Lieberzeit, P. A.; Schirk, C.; Glanznig, G.; Gazda-Miarecka, S.; Bindeus, R.; Nannen, H.; Kauling, J.; Dickert, F. L. *Superlatt. Microstruct.* **2004**, *36*, 133.
16. Colonna, M.; Berti, C.; Fiorini, M. *J. Appl. Polym. Sci.* **2014**, *131*, 39820.
17. Galloway, T.; Cipelli, R.; Guralnik, J.; Ferrucci, L.; Bandinelli, S.; Corsi, A.; Money, C.; McCormack, P.; Melzer, D. *Environ. Health Perspect.* **2010**, *118*, 1603.
18. Hattori, Y.; Iguchi, T. *Congenit. Anom.* **2004**, *44*, 125.
19. Rosenger, J. P.; Karlsson, I. G.; Nicholls, I. A. *Org. Biomol. Chem.* **2004**, *2*, 3374.
20. Sembongi, K.; Tanaka, M.; Sakurada, K.; Kobayashi, M.; Itagaki, S.; Hirano, T.; Iseki, K. *Biol. Pharm. Bull.* **2008**, *31*, 497.
21. He, P.; Cheng, X.; Staufenbiel, M.; Li, R.; Shen, Y. *PLOS One* **2013**, *8*, e55091.
22. Seidler, K.; Lieberzeit, P. A.; Dickert, F. L. *Analyst* **2009**, *134*, 361.
23. Oliveira, S. C. B.; Chiorcea-Paquim, A. M.; Ribeiro, S. M.; Melo, A. T. P.; Vivan, M.; Oliveira-Brett, A. M. *Bioelectrochemistry* **2009**, *76*, 201.
24. Kasemo, B. *Surf. Sci.* **2002**, *500*, 656.
25. Lingenfelder, M.; Tomba, G.; Costantini, G.; Ciacchi, L. C.; De Vita, A.; Kern, K. *Angew. Chem. Int. Ed.* **2007**, *46*, 4492.
26. Sauerbrey, G. *Zeitschrift für Physik* **1959**, *155*, 206.
27. Jenik, M.; Seifner, A.; Lieberzeit, P.; Dickert, F. L. *Anal. Bioanal. Chem.* **2009**, *394*, 523.
28. Heng, J. Y. Y.; Bismarck, A.; Lee, A. F.; Wilson, K.; Williams, D. R. *Langmuir* **2006**, *22*, 2760.
29. Bucton, G.; Gill, H. *Adv. Drug Del. Rev.* **2007**, *59*, 1474.
30. Furuyama, N.; Hasegawa, S.; Yada, S.; Hamaura, T.; Wakiyama, N.; Yonemochi, E.; Terada, K.; Buckton, G. *Chem. Pharm. Bull.* **2011**, *59*, 1452.
31. Jaskólski, M.; Li, M.; Laco, G.; Gustchina, A.; Alexander, W. *Acta Cryst.* **2006**, *D62*, 208.
32. Alsudir, S.; Lai, P. C. E. *Eur. Chem. Bull.* **2013**, *2*, 112.
33. Xiang, S. C.; Zhang, Z.; Zhao, C.-G.; Hong, K.; Zha, X.; Ding, D.-R.; Xie, M.-H.; Wu, C.-D.; Das, M. C.; Gill, R.; Thomas, K. M.; Chen, B. *Nature Commun.* **2011**, *204*, 114.
34. Qiu, J.; Wang, S. *J. App. Polym. Sci.* **2011**, *119*, 3670.
35. Owens, D. K.; Wendt, R. C. *J. Appl. Polym. Sci.* **1969**, *13*, 1741.
36. Li, Q.; Rudolph, B.; Weigl, B.; Earl, A. *Int. J. Pharm.* **2004**, *280*, 77.
37. Feynman, R. P. In Miniaturization, Gilbert, H. D., Ed.; Reinhold: New York, **1961**, pp 282.
38. Diltemiz, S. E.; Hür, D.; Ersöz, A.; Denizli, A.; Say, R. *Biosens. Bioelectr.* **2009**, *25*, 599.
39. Mamdough, W.; Uji, H.; Gesquiére, A.; Feyter, S. D.; Amabilino, D. B.; Abdel-Mottaleb, M. M. S.; Veciana, J.; De Schryver, F. C. *Langmuir* **2004**, *20*, 9628.
40. Dickert, F. L.; Haunschild, A.; Kuschow, V.; Reif, M.; Stathopoulos, H. *Anal. Chem.* **1996**, *68*, 1058.
41. Fielden, M. R.; Brennan, R.; Gollub, J. *Toxicol. Sci.* **2007**, *99*, 90.
42. Lieberzeit, P. A.; Halikias, K.; Afzal, A.; Dickert, F. L. *Anal. Bioanal. Chem.* **2008**, *392*, 1405.
43. Ho, R.; Heng, J. Y. Y.; Dilworth, S. E.; Williams, D. R. *J. Adhesion* **2008**, *84*, 483.
44. Edelstein, S. J.; Changeux, J. P. *Biophys. J.* **2010**, *98*, 2045.